

Hiroki Ohta · Shin-ichi Sasa

Jamming transition in kinetically constrained models with reflection symmetry

Abstract A class of kinetically constrained models with reflection symmetry is proposed as an extension of the Fredrickson-Andersen model. It is proved that the proposed model on the square lattice exhibits a freezing transition at a non-trivial density. It is conjectured by numerical experiments that the known mechanism of the singular behaviors near the freezing transition in a previously studied model (spiral model) is not responsible for that in the proposed model.

Keywords Lattice theory and statistics · Theory and modeling of the glass transition · Percolation

PACS 05.50.+q · 64.70.Q- · 64.60.ah

1 Introduction

Athermal particles with repulsive interactions exhibit rigidity with an amorphous structure when the density of the particles is higher than a critical value. Such a phenomenon is referred to as a *jamming transition*, and elucidation of the nature of jamming transitions is a challenging problem in statistical physics [1,2,3,4,5,6,7,8]. Thus far, the replica theories and the related cavity methods for equilibrium glass models have provided insights into jamming transitions as well as glass transitions [9,10]. As a different approach, kinetically constrained models (KCMs), which were investigated with a physical picture that glassy dynamics is purely kinematic [11,12,13], have been considered for understanding jamming transitions [14]. A particular property of KCMs is the absence of singularities in the equilibrium properties. Nevertheless, dynamical phase transitions in KCMs on Bethe lattices have been known to be strongly connected to a certain dynamical phase transition called a freezing transition in equilibrium glass models [15]. Also, recent studies have attempted to reveal the relationship between KCMs and glass-forming materials [16,17].

Let us review theoretical studies on KCMs in brief. Here, we generally call dynamical phase transitions in KCMs freezing transitions, which mean the transition from an equilibrium phase to a frozen phase where an infinite number of particles are at rest as a result of blocking by other particles. The first proof for the existence of a freezing transition was presented for the Fredrickson-Andersen (FA) model and then also the Kob-Andersen model on a Bethe lattice [18,19]. However, for these models in finite dimensions, it has been shown that there are no true phase transitions [19,20], even though the numerical simulations have shown an indication of a transition. Then, it has been proved that a KCM, which is called spiral model, exhibits a freezing transition in two dimensions [21,22], leading to the concept of universality classes (we call that of the spiral model *spiral class*) for finite-dimensional freezing transitions.

Hiroki Ohta
Yukawa Institute for Theoretical Physics, Kyoto University, Kyoto 606-8502, Japan
E-mail: Hiroki.Ohta@nbi.dk
Niels Bohr Institute/NBIA, University of Copenhagen, Copenhagen 2100, Denmark

Shin-ichi Sasa
Department of Physics, Kyoto University, Kyoto 606-8502, Japan

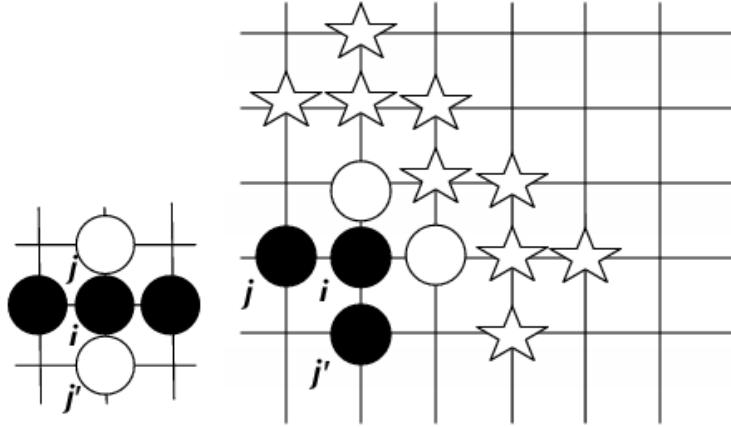


Fig. 1 Two configurations satisfying $\sum_{j \in B_i} \sigma_j = 2$. In the configuration to the left, the particle at site i is constrained, because f_j and $f_{j'}$ are at most 1. In the configuration to the right, the particle at site i is not constrained only when there are no particles at the sites marked with the star symbol. The particle at site i becomes constrained when a particle is placed at the sites marked with the star symbol.

However, the meaning of such a concept of universality classes for KCMs, in particular, in finite dimensions has not been deeply understood because the spiral model is somewhat an ideally simple case that does not have reflection symmetry, and the classes different from the *spiral* class have not been known yet. Thus, the previous studies have attempted to estimate the universality classes in the other models: a finite-size scaling analysis using a special boundary condition for the knight model is consistent to the *spiral* class [23], and the robustness of the universality against two (periodic and filled) boundary conditions for a wider class of models showing the freezing transition in finite dimensions has been investigated, which leads that the universality class of investigated models in two dimensions also looks consistent to the *spiral* model [24] although the numerical data are not as conclusive as that with using a special boundary condition [23]. Therefore, it is a significant challenge to present a KCM that exhibits a freezing transition but does not belong to the *spiral* class. We attempt to solve this problem.

In particular, we focus on KCMs with reflection symmetry, which may be conjectured as qualitatively different from KCMs in the *spiral* class owing to the symmetry of the models. We also search for models, which in their mean-field cases such as the models on the infinite dimensional lattice and Bethe lattices are straightforwardly well-defined. Mean-field analysis for such cases possibly acts as a starting point for a theory on determining the universality, as we have learned from the renormalization group analysis for equilibrium critical phenomena. With this background, the strategy in this paper is to first remind us of the FA model, which is straightforwardly well-defined on Bethe lattices but does not show any freezing transitions in finite dimensions. Then, by adding the other constraints to the FA model, we propose a KCM with reflection symmetry, for which the existence of a freezing transition can be proved on the square lattice. Further, we conjecture by numerical experiments that the proposed model does not belong to the *spiral* class.

2 Model

Let Λ be a square lattice consisting of sites $i \equiv (i_x, i_y)$, where i_x and i_y are integers satisfying $1 \leq i_x \leq L$ and $1 \leq i_y \leq M$, where $M = L$ is assumed unless otherwise specified. We define the occupation variable $\sigma_i \in \{0, 1\}$ at each site $i \in \Lambda$, and assume a Hamiltonian

$$H(\sigma) = \sum_{i \in \Lambda} \sigma_i, \quad (1)$$

where we express $\sigma \equiv (\sigma_i)_{i \in \Lambda}$ collectively. Concretely, $\sigma_i = 1$ represents a state that a particle occupies site i , while there is no particle at site i when $\sigma_i = 0$. In the argument below, we assume that particles are filled outside of the system, which we call the filled boundary condition, unless otherwise specified. In fact, in numerical experiments at section 4.1, we use the periodic boundary condition where sites $\{L, y\}$ and $\{x, L\}$ are connected to $\{1, y\}$ and $\{x, 1\}$ for any x and y , respectively; also, at section 4.2, we use the half-filled

boundary condition that particles are filled in the left and right region of the outside of the system, while no particles exist in the top and bottom region of the outside of the system. We consider a Markov stochastic process with a transition ratio $R(\sigma \rightarrow \sigma')$ for $\sigma \neq \sigma'$. Let $P(\sigma, t)$ be the probability distribution of a particle configuration σ at time t . The time evolution of $P(\sigma, t)$ obeys

$$\partial_t P(\sigma, t) = \sum_{\sigma' \neq \sigma} [R(\sigma' \rightarrow \sigma)P(\sigma', t) - R(\sigma \rightarrow \sigma')P(\sigma, t)]. \quad (2)$$

In this work, we study a constrained Glauber dynamics, where the transition ratio $R(\sigma \rightarrow \sigma')$ is written as

$$R(\sigma \rightarrow \sigma') = \sum_i \delta(\sigma', F_i \sigma) r(\sigma \rightarrow \sigma') \mathcal{C}_i(\sigma). \quad (3)$$

We explain the right-hand side of the equation in order. First, F_i is the creation and annihilation operator described by

$$(F_i \sigma)_j = (1 - \sigma_i) \delta_{ij} + \sigma_j (1 - \delta_{ij}). \quad (4)$$

The term $\delta(\sigma', F_i \sigma)$ represents a rule that the transition is caused by a particle creation or annihilation at each site. The term $r(\sigma \rightarrow \sigma')$ is given as

$$r(\sigma \rightarrow \sigma') = \min \left[1, \exp \left(\frac{H(\sigma) - H(\sigma')}{T} \right) \right], \quad (5)$$

where it satisfies

$$\frac{r(\sigma \rightarrow \sigma')}{r(\sigma' \rightarrow \sigma)} = \exp \left(-\frac{H(\sigma') - H(\sigma)}{T} \right), \quad (6)$$

and the Boltzmann constant is set to unity. Finally, with regard to the function $\mathcal{C}_i(\sigma)$, $\mathcal{C}_i(\sigma) = 0$ specifies a set of configurations for which particle creation and annihilation at site i is prohibited, and $\mathcal{C}_i(\sigma) = 1$, for the other configurations. We also assume that $\mathcal{C}_i(\sigma)$ is independent of σ_i .

It should be noted that the canonical distribution with the Hamiltonian (1) is the stationary solution of (2) with (3) because the transition ratio (3) satisfies the detailed balance condition. Therefore, there are no equilibrium phase transitions in the system. Nevertheless, it has been shown that there is a certain dynamical transition (freezing transition) for an appropriately selected $\mathcal{C}_i(\sigma)$. In all examples known thus far, $\mathcal{C}_i(\sigma)$ are described by using the oriented structure of the lattice [14, 21, 22, 23, 24]. In this paper, we generally assume that $\mathcal{C}_i(\sigma)$ is a reflection-symmetric function satisfying $\mathcal{C}_i(\sigma) = \mathcal{C}_i(\mathcal{P}_i^w \sigma)$ for $\forall i$ and any possible w where a configuration $\mathcal{P}_i^w \sigma$ is given by the reflection of σ with respect to the axis with angle w from the x axis. Note that w takes $0, \pi/4, \pi/2$, and $3\pi/4$ in the case of the square lattice: for example, $\mathcal{P}_i^0 \sigma_{i_x, i_y+d} = \sigma_{i_x, i_y-d}$ and $\mathcal{P}_i^{\pi/4} \sigma_{i_x-d, i_y+d} = \sigma_{i_x+d, i_y-d}$ for any integer d , and also in order to keep consistency in the cases of the filled and half-filled boundary condition, there are assumed to be sites on the infinite square lattice in the outside of the system.

From now, we explain our selection of $\mathcal{C}_i(\sigma)$. We first define

$$f_i \equiv \sum_{j \in B_i} \delta(\sigma_j, 0) \left[\prod_{\ell \in B_j} \delta(\sigma_\ell, 0) \right], \quad (7)$$

where B_i is a set of the nearest neighbor sites of site i and $\delta(m, n)$ represents Kronecker's delta function. f_i represents the number of empty sites j in B_i such that there are no particles next to any site j . From this definition, we find $f_i = 0$ for site i with a particle. Then, we set $\mathcal{C}_i(\sigma) = 0$ when $\sum_{j \in B_i} \sigma_j \geq k$ and

$$\sum_{j \in B_i} \Theta(f_j - c/2) < c/2, \quad (8)$$

where c is the connectivity of the lattice, $0 \leq k \leq c$, and $\Theta(x)$ is a step function such that $\Theta(x) = 1$ for $x \geq 0$, otherwise $\Theta(x) = 0$. It should be noted that $c = 4$ for the square lattice. For the square lattice, one can immediately find that there are no freezing transitions for all the values of k without condition (8) because these are identical to the FA models [19, 20]. Moreover, the cases without condition (8) are identical to those with condition (8) for $k = 3, 4$. On the other hand, owing to condition (8), the behaviors for the cases of

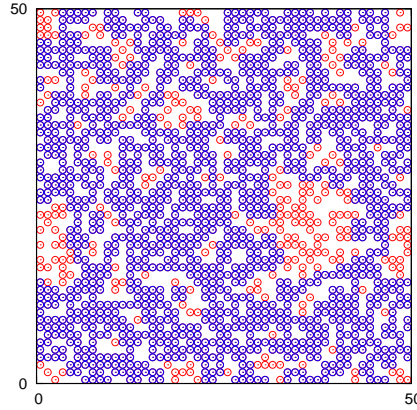


Fig. 2 (Color online) A particle configuration at an initial condition with $L = 50$, the periodic boundary, and $\rho = 0.69$: Blue points are frozen particles and red points are unfrozen particles.

$k = 0, 1, 2$ become nontrivial. We explain condition (8) with $k = 2$ through the following examples. In this paper, we consider only this simple and nontrivial case with $k = 2$, and we say that *the particle at site i is constrained* when $\mathcal{C}_i(\sigma) = 0$ and $\sigma_i = 1$.

First, one can find easily that a particle at site i is constrained if $\sum_{j \in B_i} \sigma_j = 3$ and 4. More complicated situations occur at $\sum_{j \in B_i} \sigma_j = 2$. In figure 1, for the particle at site i , there are two cases satisfying the condition $\sum_{j \in B_i} \sigma_j = 2$. In the configuration to the left in figure 1, f_j and $f_{j'}$ for the empty sites j and j' are at most 1, leading to $\sum_{j \in B_i} \Theta(f_j - 2) = 0$. Therefore, in this case, the particle at site i is constrained. On the other hand, in the configuration to the right in figure 1, only when there are no particles at the sites marked with the star symbol, f_j and $f_{j'}$ for the empty sites j and j' are 2, leading to $\sum_{j \in B_i} \Theta(f_j - 2) = 2$. In this case, the particle at site i is not constrained. When at least one particle is placed at the sites marked with the star symbol, $\sum_{j \in B_i} \Theta(f_j - 2) = 1$, which means that the particle at site i is constrained as the result. Using similar considerations, one can also find that the function $\mathcal{C}_i(\sigma)$ is independent of σ_i and the reflection symmetry condition $\mathcal{C}_i(\sigma) = \mathcal{C}_i(\mathcal{P}_i^w \sigma)$ holds for $\forall i$ and any possible w .

In this work, we focus on the relaxation behaviours of the system from an initial state, where sites are randomly occupied with a probability ρ . Moreover, as the simplest case, we consider the zero temperature limit $T \rightarrow 0$. The equilibrium state in this case involves no particles. Now, let us suppose that a particle configuration at $t = 0$ contains a set of particles constrained by only constrained particles and boundary sites. Such particles are referred to as *frozen particles*. As a reference, we show a configuration of frozen particles in figure 2. Since frozen particles cannot annihilate, they can never reach the equilibrium state. On the other hand, when no frozen particles exist at $t = 0$, all the particles annihilate, and hence, the final state becomes the equilibrium state. In this manner, whether a *freezing* transition, which is a phase transition between equilibrium states and such frozen states, occurs is determined by investigating the existence of frozen particles in initial configurations.

3 Existence of a freezing transition

In this section, we prove that a freezing transition occurs at a certain value $0 < \rho_c < 1$ in the proposed model. In concrete terms, we show that there is a density $\rho_l > 0$, below which the probability of finding frozen particles at the bulk in initial configurations goes to zero in the thermodynamic limit, while there is a density $\rho_u < 1$, above which frozen particles can be found in initial configurations with probability one in the thermodynamic limit. By estimating such a lower bound ρ_l and an upper bound ρ_u of the transition point ρ_c , we may conclude that $0 < \rho_l \leq \rho_c \leq \rho_u < 1$.

3.1 Equilibrium states at $\rho < \rho_l$

Let us estimate a lower bound below which the probability of finding frozen particles at the bulk goes to zero in the thermodynamic limit. Specifically, let us consider whether the particle at centered site $(L/2, L/2)$,

which is a representation of the bulk, is frozen. First, we assume that the clusters of frozen particles in the bulk are always constrained partly by the boundary sites (See Appendix for the sketch of the proof). Therefore, the minimum number of frozen particles including this centered site is more than $L/3$, because each frozen particle in one frozen cluster has to be located at a site within distance 3 from another frozen particle by the definition, and also such a sequence of the frozen particles has to percolate from one boundary and another boundary with length L .

Concretely, let $(i^{(k)})_{k=1}^N$ be a sequence of N -sites such that (0) $\exists k$ satisfying $k = (L/2, L/2)$ (i) $\sigma_{i^{(k)}} = 1$ for $\forall k$, (ii) $0 < |i^{(k)} - i^{(k+1)}| \leq 3$ for $\forall k$ (iii) $|i^{(k)} - i^{(k')}| > 3$ for $\forall k$ and $\forall k' \neq k \pm 1$ where the distance between site i and j is denoted by $|i - j| \equiv |i_x - j_x| + |i_y - j_y|$. Note that (ii) and (iii) lead to (iv) $i^{(k_1)} \neq i^{(k_2)}$ for $\forall k_1$ and $\forall k_2 \neq k_1$. For a given configuration σ , we define a set of all such sequences, which is denoted by $\mathcal{D}_N(\sigma)$. From the fact mentioned above, we can always find a sequence of sites in $\mathcal{D}_{L/3}(\sigma)$ if frozen particles including the centered site are present in the initial configuration σ , where $L/6$ is assumed to be an integer without loss of generality. Thus, the probability Q of finding a frozen particle at the centered site in initial configurations satisfies

$$Q \leq \text{Prob}(\mathcal{D}_{L/3} \neq \emptyset). \quad (9)$$

Here, we also obtain

$$\text{Prob}(\mathcal{D}_{L/3} \neq \emptyset) \leq \text{Prob}(\exists (i_*^{(k)})_{k=1}^{L/3}), \quad (10)$$

where $(i_*^{(k)})_{k=1}^{L/3}$ satisfies conditions (0), (i), (ii), and (iv) that is weaker than (iii). Further, by recalling the conditions (0) and (iv), we easily obtain $\text{Prob}(\exists (i_*^{(k)})_{k=1}^{L/3}) \leq W^{L/6-1}$, where $W \equiv \sum_{i:0 < |i-j| \leq 3} \text{Prob}(\sigma_i = 1 | \sigma_j = 1) = 24\rho$. These estimations give

$$Q \leq (24\rho)^{L/6-1}. \quad (11)$$

Therefore, when ρ is less than $1/24$, $Q \rightarrow 0$ in the thermodynamic limit. The obtained results can be applied to the sites which are sufficiently far from the boundaries. We thus find a lower bound as $\rho_l = 1/24$.

3.2 Frozen states at $\rho > \rho_u$

Let \mathcal{B} be a set of directed bonds written as $\{(4k, 2l) \rightarrow (4k+2, 2l \pm 1)\}$ or $\{(4k-2, 2l+1) \rightarrow (4k, 2l+1 \pm 1)\}$, where $k, l \in \mathbb{Z}$. We say that a bond $\{(n, m) \rightarrow (n+2, m \pm 1)\} \in \mathcal{B}$ is occupied when three sites $(n+1, m)$, $(n+2, m)$, and $(n+2, m \pm 1)$ are all occupied. See the left-side of figure 3 for an example of occupied bonds. Now, if there exists an infinite connected cluster (in the sense of a directed percolation) of the occupied bonds in \mathcal{B} , we can find frozen particles in the thermodynamic limit. Thus, the problem becomes to be similar to the standard directed percolation in a cellular automaton [25]. However, the occupation of bond $\{(n, m) \rightarrow (n+2, m+1)\}$ is not independent of the occupation of bond $\{(n, m) \rightarrow (n+2, m-1)\}$ because the occupation of the two sites, $(n+1, m)$ and $(n+2, m)$, influences the two bonds. Due to this effect, it is not straightforward to obtain the explicit percolation point.

In order to overcome this difficulty, we introduce two auxiliary variables, β_i^+ and β_i^- , which take the value 0 with probability $1 - \tilde{\rho}$, and 1, with probability $\tilde{\rho}$. Then, one can find that the probability measure of σ in the initial conditions is the same as that of $(\beta_i^+ + \beta_i^- - \beta_i^+ \beta_i^-)_{i \in \Lambda}$ if $\tilde{\rho}$ satisfies $\rho = 1 - (1 - \tilde{\rho})^2$. This can simplify the present problem in the following way. Here, instead of the bond defined by the occupation variable σ_i , we consider the bond defined by the auxiliary variables β_i^\pm , as follows. As shown in figure 3, we say that a bond $\{(n, m) \rightarrow (n+2, m+1)\}$ is β -occupied when $\beta_{n+1, m}^+ = \beta_{n+2, m}^+ = \beta_{n+2, m+1}^+ = 1$. Likewise, $\{(n, m) \rightarrow (n+2, m-1)\}$ is called β -occupied when $\beta_{n+1, m}^- = \beta_{n+2, m}^- = \beta_{n+2, m-1}^- = 1$. As β -occupation for each bond independently occurs with the probability $p = \tilde{\rho}^3$, there is a critical value

$$p_c = \tilde{\rho}_c^3 \simeq 0.644 \dots, \quad (12)$$

above which the directed bond percolation occurs [25]. It can be seen that if a bond is β -occupied, the bond in the original problem, which is made by the relation $\sigma_i = \beta_i^+ + \beta_i^- - \beta_i^+ \beta_i^-$, is also occupied. Thus, an

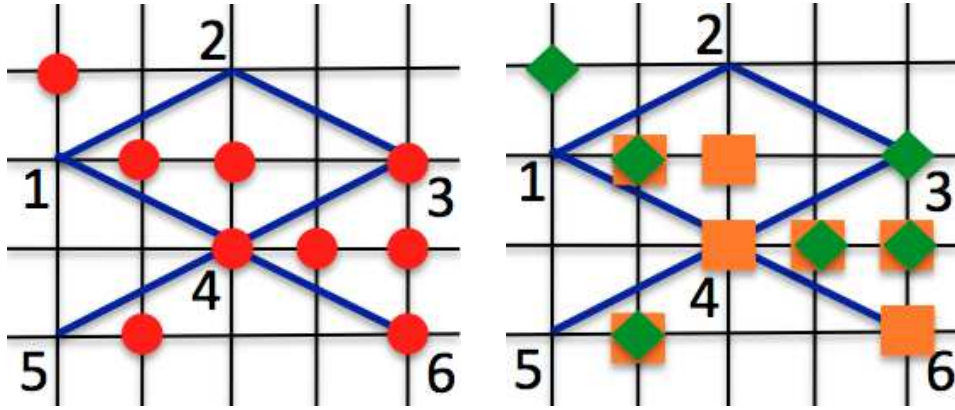


Fig. 3 (Color online) Example of bond-occupation. Three bonds $\{1 \rightarrow 4\}$, $\{4 \rightarrow 3\}$, and $\{4 \rightarrow 6\}$ are occupied in the particle configuration, where each circle symbol represents a particle in the left-side. The particle configuration in the left-side is also generated by using β^+ and β^- as illustrated in the right-side, where square and diamond symbols at each site correspond to $\beta^+ = 1$ and $\beta^- = 1$, respectively.

infinite connected cluster of β -occupied bonds indicates an infinite connected cluster of bonds in the original problem. By using the condition to recover the original problem:

$$\rho_u = 1 - (1 - \tilde{\rho}_c)^2, \quad (13)$$

we find that there exists an infinite connected cluster (in the sense of a directed percolation) of occupied bonds in \mathcal{B} for $\rho > \rho_u$. Thus $\rho_u \simeq 0.981 \dots$ is an upper bound.

4 Conjectures by numerical experiments

In this section, we numerically try to obtain a greater lower bound and a smaller upper bound of the transition point ρ_c than those given in the previous section. We also present numerical evidence that the mechanism to characterize the *spiral* class is not relevant to the freezing transition in the proposed model. The key point to obtain useful bounds for ρ_c in the model with the filled boundary condition is to introduce different boundary conditions from the filled one as explained in the following.

4.1 Greater lower bounds

Lower bounds of the transition point are numerically obtained by checking whether initial configurations with density ρ relax to the equilibrium configuration in the thermodynamic limit. In order to avoid strong finite size effects caused directly from the filled boundary, we use the periodic boundary condition on the assumption that the transition points obtained in the thermodynamic limit for both of two boundary conditions are identical. Since we do not have any proof to support this assumption, though it would make sense, the analysis below should be regarded as a reference for further studies. Specifically, we measure the relaxation time $\tau_0 \equiv \min \tau'$ such that $H(\sigma(\tau')) = 0$ as a function of ρ . As shown in figure 4, τ_0 increases when ρ is increased. Taking into account the size-dependence of τ_0 , one might estimate safely $\rho_c \geq 0.67$. It should be noted that a longer simulation time and also smarter algorithms would allow us to obtain better estimations of lower bounds for ρ_c . Here, the rather important point is that a reliable finite-size scaling form of τ_0 was not found as far as we studied. One possibility for it might be that τ_0 obeys a Vogel-Fulcher type singularity as found in the spiral model [21].

4.2 Smaller upper bounds and the absence of the *spiral* universality class

Next we attempt to find smaller upper bounds of the transition point. In order to investigate the behaviors in high densities, we introduce a half-filled boundary condition that particles are filled in the left and right

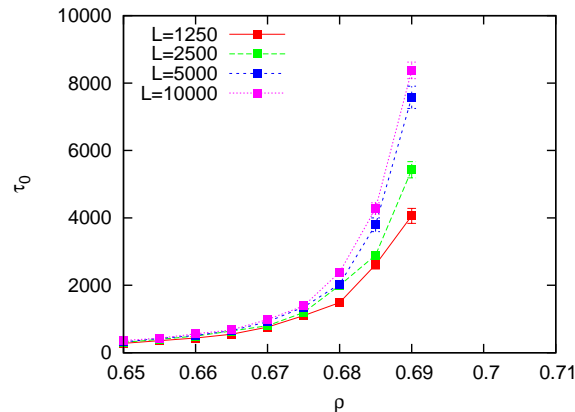


Fig. 4 (Color online) Relaxation time τ_0 with different system size L .

region of the outside of the system, while no particles exist in the top and bottom region of the outside of the system. Then, we try to observe a percolation of frozen particles in the direction from left to right under this half-filled boundary condition. In fact, if such a directed percolation occurs in the case of the half-filled boundary condition, the corresponding frozen particles would be observed in the system with the filled boundary conditions. As we will see, one can detect a part of frozen particles with the filled boundary condition in high densities using the half-filled boundary condition.

First, we estimate the probability $P_L(\rho)$ of finding a percolating frozen cluster, in which there is no i'_x such that $\sigma_{i'_x-1, i_y} = \sigma_{i'_x, i_y} = \sigma_{i'_x+1, i_y} = 0$ for arbitrary i_y for the half-filled boundary condition with $M = L^{1/z}$. We may restrict our investigation to $0 \leq z^{-1} \leq 1$ because of the $\pi/2$ rotational symmetry in the system with the filled boundary condition. Then, for an assumed value of z , we determine whether a density ρ_{dp} exists such that $\lim_{L \rightarrow \infty} P_L(\rho) = \Theta(\rho - \rho_{dp})$ where Θ is the step function defined before. If such a density ρ_{dp} exists, it corresponds to a directed percolation point for the system modified with $M = L^{1/z}$. In this manner, we can determine a set of values (ρ_{dp}, z) , and ρ_{dp} provides an upper bound of the transition point. Practically, in numerical experiments, for a given value of z , we consider a cross point of the two curves $P_{L/2}(\rho)$ and $P_L(\rho)$, which is denoted by $\rho_{cr}^L(z^{-1})$. We then check whether $\rho_{cr}^L(z^{-1}) \rightarrow \rho_{dp}$ in the limit $L \rightarrow \infty$.

In this way, we consider the possibility of finding a convergence point ρ_{dp} with $z^{-1} = 0.63$ where the criticality of the *spiral* class possibly appears. As shown in the left side of figure 5, the numerical data up to $L = 4000$ suggest that ρ_{cr}^L are scattered to judge convergence to a special value where the density is changed by an increment of 0.0005. At this stage, there are two possibilities; one is that there is no convergence point in this procedure with $z^{-1} = 0.63$, and the other is that we may find the existence of ρ_{dp} by studying larger system sizes. The first case means that the freezing transition is not connected to the exponent $z^{-1} = 0.63$. That is, the freezing transition in our model does not belong to the *spiral* class. We now elaborate on the second possibility by employing a different method, finite-size scaling analysis $P_L(\rho)$. As shown in figure 6, the finite-size scaling analysis with the exponents of the standard directed percolation provides reasonable collapsed data with a fitting density $\rho_{fit} = \rho_{fit}^0$, which could be a plausible estimation for ρ_{dp} . (Although we tried to collapse the data with different values of ρ_{fit} , the manner of the collapse with, for example, $\rho_{fit} = 0.723$ was definitely worse than that for $\rho_{fit} = \rho_{fit}^0$.) However, even in this case, we conjecture that the freezing transition in our model does not belong to the *spiral* class by the following reason: As shown in the right side of figure 5, we have found much better convergences for $z^{-1} = 0.68$ with a convergence point ρ_{dp} , which is smaller than $\rho = 0.723$. This means that ρ_{dp} for $z^{-1} = 0.68$ may be another smaller upper bound than $\rho_{fit} = \rho_{fit}^0$, and that the properties at this smaller upper bound may be characterized by a different value from $z^{-1} = 0.63$. Thus, this upper bound $\rho_{fit} = \rho_{fit}^0$ is not relevant to the transition point of the model with the filled boundary condition. In other words, if we perform similar experiments for the spiral model removing particles from the boundaries in a proper way [23], where boundaries are $\pi/4$ -angle rotated from the present half-filled boundaries, $\rho_{fit} = \rho_{dp}(z^{-1})$ should hold for $\forall z$ satisfying $z^{-1} > 0.63$ because no other percolating (frozen) cluster except for the ones made by the standard cellular automaton exist in the system with such half-filled boundaries. This fact is completely different from the obtained results here. In sum, for both the

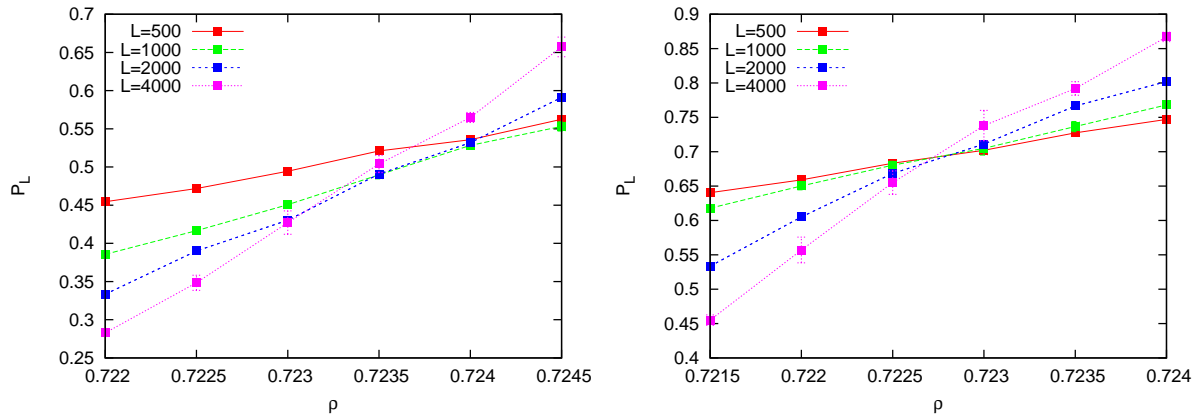


Fig. 5 (Color online) $P_L(\rho)$ for $z^{-1} = 0.63$ (left) and 0.68 (right).

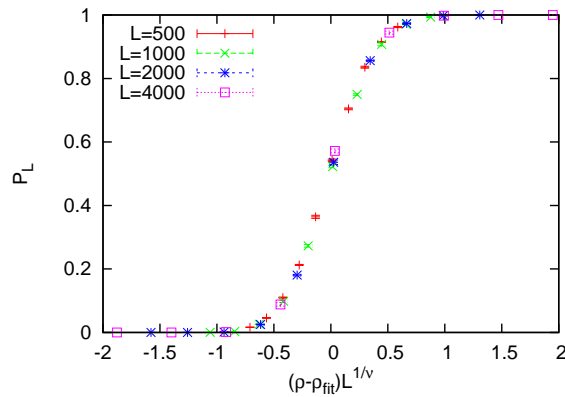


Fig. 6 (Color online) Finite-size scaling of $P_L(\rho)$ with $z^{-1} = 0.63$ and $\nu = 1.7338$ [23]. We used $\rho_{\text{fit}} = \rho_{\text{fit}}^0 \equiv 0.7237$.

two possibilities, these numerical results lead to a conclusion that the freezing transition in the proposed model does not belong to the *spiral* class.

One may point out a possibility that the diagonally half-filled boundary condition that was used for the previous study [23] provides a nontrivial upper bound which is responsible for the *spiral* class of the transition in the knight model with the filled boundary condition. Here, the diagonally half-filled boundary condition means that the states of sites along four diagonal lines for the lattice are fixed as boundary sites, having particles for one facing pair of two lines and no particles for the other pair. However, we have numerically observed that the percolation density for the present model with the diagonally half-filled boundary condition is very close to 1 even if it exists, which is reasonable by considering the properties of the constraint function. Therefore, the present model with the diagonally half-filled boundary does not have any possibilities to be connected to the *spiral* class of the transition in the model with the filled boundary condition. Thus, as we have discussed above, we have considered this possibility for the model with the present half-filled boundary condition.

As a reference, we report tentative numerical results for the dependence of $P_L(\rho)$ on z^{-1} from the other viewpoint. We quantitatively investigate the extent of the convergence by measuring the average value of the cross points $\bar{\rho}_{\text{cr}} \equiv \sum_{i=1}^3 \rho_{\text{cr}}^{L_i} / 3$ with $L_i = 500 \times 2^i$ and the deviation $\Delta \rho_{\text{cr}} \equiv \sqrt{\sum_{i=1}^3 (\rho_{\text{cr}}^{L_i} - \bar{\rho}_{\text{cr}})^2 / 3}$ for each value of z^{-1} . Further, we estimated $\rho_{\text{cr}}^{L_i}$ by approximating $P_L(\rho)$ as a piece-wise linear function. When $\Delta \rho_{\text{cr}}$ is sufficiently small, we expect an obvious convergence of $\rho_{\text{cr}}^{L_i}$ in the limit $L \rightarrow \infty$. Figure 7 presents the numerical results of $\Delta \rho_{\text{cr}}$ for $0.63 \leq z^{-1} \leq 0.78$, where $\Delta \rho_{\text{cr}}$ exhibits an oscillatory behaviour with local minima at $z^{-1} = 0.64, 0.68, 0.73$, and 0.75 . Assuming that $\bar{\rho}_{\text{cr}}$ at such local minima can be regarded as ρ_{dp} , we show the z -dependence of ρ_{dp} in figure 7. Further, this leads us to guess that there are such local minima

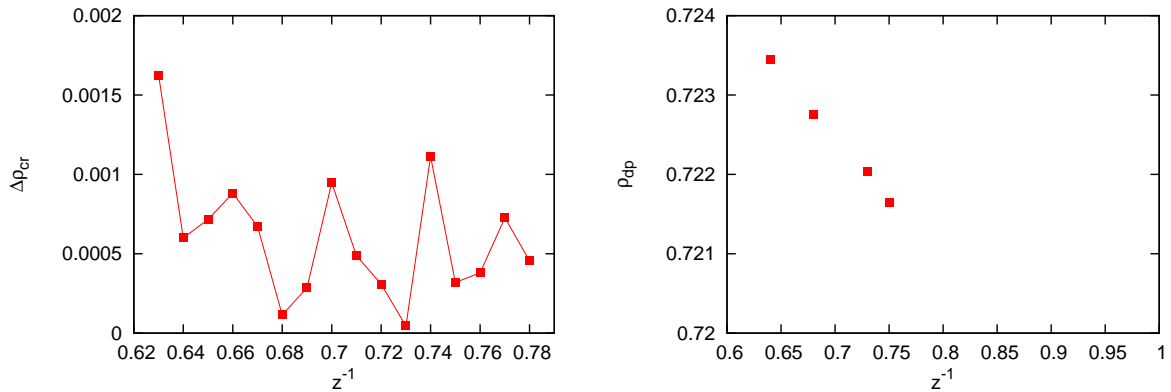


Fig. 7 (Color online) $\Delta\rho_{cr}$ as a function of z^{-1} (left). ρ_{dp} as $\bar{\rho}_{cr}$ for $z^{-1} = 0.64, 0.68, 0.73,$ and 0.75 (right).

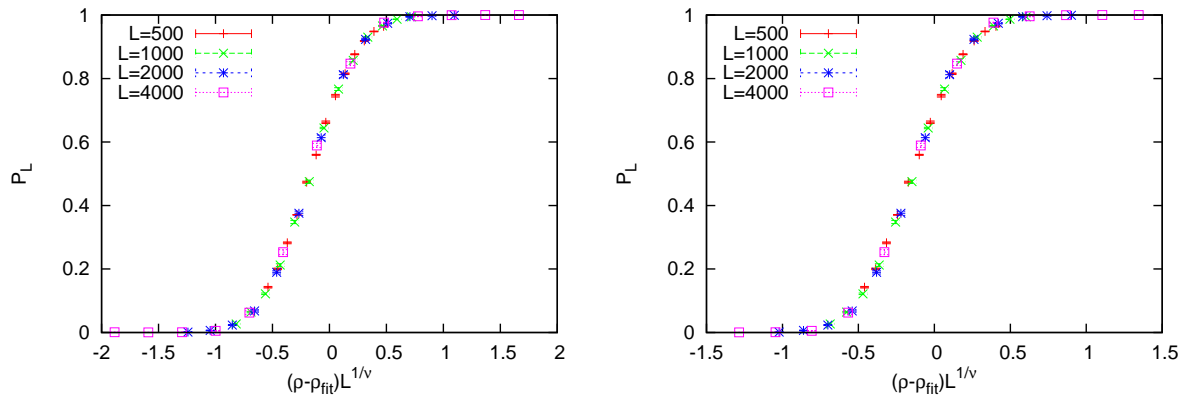


Fig. 8 (Color online) Finite-size scaling of P_L for $z^{-1} = 0.68$. $\nu = 1.66$ (left) and $\nu = 1.7338$ (right). $\rho_{fit} = 0.72275$.

points in $\Delta\rho_{cr}$ at larger values of z^{-1} even though it is not easy to obtain them numerically due to the longer numerical simulations required. Therefore, in principle, there exists the smallest upper bound ρ_{dp*} that can be obtained by this procedure as $\rho_c \leq \rho_{dp*} \leq 0.7217(5) < \rho_{fit}^0$. The possible interpretation of an oscillatory behaviour in $\Delta\rho_{cr}$ is the coexistence of different cellular automaton making distinct directed percolating (frozen) clusters, each of which is characterized by different exponents z at different percolation densities ρ_{dp} . This interpretation is not very unreasonable because one can easily construct another cellular automaton making frozen clusters at the high densities in the model with the filled boundary condition, which is different from the cellular automaton introduced in the section 3.2. Further, we have performed the finite-size scaling of P_L also for $z^{-1} = 0.68$ using ρ_{dp} estimated above with ν as a fitting parameter as shown in the left-hand side of figure 8. At least, the fitting with $\nu = 1.66$ supports the existence of a universal curve. Note that it is not very easy to estimate the best fitting value of ν : for example, the fitting with $\nu = 1.7338$ would be still reasonable as shown in the right-hand side of figure 8. However, independent of the fitting value of ν , both of the cases are also consistent with our interpretation because $z^{-1} = 0.68$ is already different from that of the spiral universality. Unfortunately, extensive numerical simulations in order to exactly answer whether our interpretation for the numerical results is correct remain to be performed in the future.

5 Concluding remarks

The main achievement of this work is the presentation of a KCM with the reflection symmetry that exhibits a freezing transition on the square lattice. Further, we conjecture by numerical experiments that the singular behaviour at the freezing transition does not belong to the *spiral* class [21,22]. Lastly, we comment on future studies in the following text.

First, the characterization of the singular behaviour near the freezing transition in our model remains to be solved. More precise estimations for the transition point ρ_c need to be derived theoretically and numerically. In particular, it might be interesting if one explicitly constructs a directed percolation problem related to the behavior near the transition point. Furthermore, the manner of divergence of the relaxation time τ_0 should be clarified. We conjecture that τ_0 in our model exhibits a Vogel-Fulcher type singularity when ρ approaches ρ_c from below, in a manner similar to that in the *spiral* class. Presently, we do not have clear evidence for the conjecture, because ρ_c has not been estimated with sufficient accuracy as yet. After obtaining precise estimations for ρ_c , we will be able to validate our conjecture by numerical experiments. Second, the theoretical analysis of the model on a Bethe lattice will be performed in order to enhance the understanding of the universality of freezing transitions in KCMs. A concrete question on Bethe lattices is whether the singular behaviour of the freezing transitions observed here can be characterized by power-law exponents associated with a mode-coupling equation, as discussed in the Fredrickson-Andersen model [18,26,27,28,29,30,31]. If the answer is yes, since it is different from the Vogel-Fulcher type singularity, we will clarify the origin of the difference between the behaviours of the model on the Bethe lattice and on the square lattice. Lastly, we would like to mention another dynamics in an equilibrium situation with a fixed average of the density [22]. The freezing transition is unchanged by the definition of the frozen particles even in this case. However, strictly speaking, we have not fully understood the effects of unfrozen particles in this case, which remain to be clarified in the future. By addressing the points above, we wish to understand how freezing transitions in KCMs are related, or unrelated, to jamming transitions.

Acknowledgements The authors thank H. Tasaki for providing us with a basic idea for the proof of the existence of a freezing transition. We also thank C. Toninelli and G. Biroli for their discussions on the numerical simulations. This work was supported by the JSPS Core-to-Core Program “International research network for nonequilibrium dynamics of soft matter”.

References

1. O’Hern C.S., Silbert L. E., Liu A. J., Nagel S. R.: Jamming at zero temperature and zero applied stress: The epitome of disorder. *Phys. Rev. E* **68**, 011306 (2003)
2. Ellenbroek W. G., Somfai E., van Hecke M., van Saaloos W.: Critical Scaling in Linear Response of Frictionless Granular Packings near Jamming. *Phys. Rev. Lett.* **97**, 258001 (2006)
3. Olsson P., Teitel S.: Critical Scaling of Shear Viscosity at the Jamming Transition. *Phys. Rev. Lett.* **99**, 178001 (2007)
4. Hatano T.: Growing length and time scales in a suspension of athermal particles. *Phys. Rev. E* **79**, 050301 (2009)
5. Otsuki M., Hayakawa H.: Critical behaviors of sheared frictionless granular materials near the jamming transition. *Phys. Rev. E* **80**, 011308 (2009)
6. Lechenault F., Dauchot O., Biroli G., Bouchaud J. P.: Critical scaling and heterogeneous superdiffusion across the jamming/rigidity transition of a granular glass. *Europhys. Lett.* **83**, 46003 (2008)
7. Candelier R., Dauchot O., Biroli G.: Building Blocks of Dynamical Heterogeneities in Dense Granular Media. *Phys. Rev. Lett.* **102**, 088001 (2009)
8. Lechenault F., Candelier R., Dauchot O., Bouchaud J. P., Biroli G.: Super-diffusion around the rigidity transition: Lévy and the Lilliputians. *Soft Matter* **6**, 3059 (2010)
9. Parisi G., Zamponi F.: Mean-field theory of hard sphere glasses and jamming. *Rev. Mod. Phys.* **82**, 789 (2010)
10. Mézard M., Parisi G., Tarzia M., Zamponi F.: On the solution of a ‘solvable’ model of an ideal glass of hard spheres displaying a jamming transition. *J. Stat. Mech.* P03002 (2011)
11. Fredrickson G. H., Andersen H. C.: Kinetic Ising Model of the Glass Transition. *Phys. Rev. Lett.* **53**, 1244 (1984)
12. Kob W., Andersen H. C.: Kinetic lattice-gas model of cage effects in high-density liquids and a test of mode-coupling theory of the ideal-glass transition *Phys. Rev. E* **48**, 4364 (1993)
13. Ritort F., Sollich P.: Glassy dynamics of kinetically constrained models. *Adv. Phys.* **52**, 219 (2003)
14. Toninelli C., Biroli G., Fisher D. S.: Jamming Percolation and Glass Transitions in Lattice Models. *Phys. Rev. Lett.* **96**, 035702 (2006)
15. Semerjian G.: On the freezing of variables in random constraint satisfaction problems. *J. Stat. Phys.* **130**, 251 (2008)
16. Candelier R., Dauchot O., Biroli G.: Dynamical facilitation decreases when approaching the granular glass transition. *Europhys. Lett.* **92**, 24003 (2010)
17. Keys A. S., Hedges L. O., Garrahan J. P., Glotzer S. C., Chandler D.: Excitations Are Localized and Relaxation Is Hierarchical in Glass-Forming Liquids. *Phys. Rev. X* **1**, 021013 (2011)
18. Sellitto M., Biroli G., Toninelli C.: Facilitated spin models on Bethe lattice: Bootstrap percolation, mode-coupling transition and glassy dynamics. *Europhys. Lett.* **69**, 496 (2005)
19. Toninelli C., Biroli G., Fisher D. S.: Cooperative Behavior of Kinetically Constrained Lattice Gas Models of Glassy Dynamics. *J. Stat. Phys.* **120**, 167 (2005)
20. Toninelli C., Biroli G., Fisher D. S.: Spatial Structures and Dynamics of Kinetically Constrained Models of Glasses. *Phys. Rev. Lett.* **92**, 185504 (2004)
21. Toninelli C., Biroli G.: A new class of cellular automata with a discontinuous glass transition. *J. Stat. Phys.* **130**, 83 (2008)
22. Biroli G., Toninelli C.: Spiral model, jamming percolation and glass-jamming transitions. *Eur. Phys. J. B* **64**, 567 (2008)
23. Toninelli C., Biroli G., Fisher D. S.: Toninelli, Biroli, and Fisher Reply:. *Phys. Rev. Lett.* **98**, 129602 (2007)

-
24. Jeng M., Schwarz J. M.: Force-balance percolation Phys. Rev. E **81**, 011134 (2010)
 25. Hinrichsen H.: Non-equilibrium critical phenomena and phase transitions into absorbing states. Adv. Phys. **49**, 815 (2000)
 26. Jäckle J., Sappelt D.: Test of analytical approximations for kinetic Ising models with sharp blocking transition. Physica A **192**, 691 (1993)
 27. Kawasaki K.: Irreducible memory function for dissipative stochastic systems with detailed balance. Physica A **215**, 61 (1995)
 28. Pitts S. J., Young T., Andersen H. C.: Facilitated spin models, mode coupling theory, and ergodic-nonergodic transitions. J. Chem. Phys. **113**, 8671 (2000)
 29. Sellitto M., Martino D. D., Caccioli F., Arenzon J. J.: Dynamic Facilitation Picture of a Higher-Order Glass Singularity. Phys. Rev. Lett. **105**, 265704 (2010)
 30. Ohta H.: Systematic perturbation approach for a dynamical scaling law in a kinetically constrained spin model. J. Stat. Mech. P01032 (2011)
 31. Franz S., Sellitto M.: Finite-size critical fluctuations in microscopic models of mode-coupling theory. J. Stat. Mech. P02025 (2013)

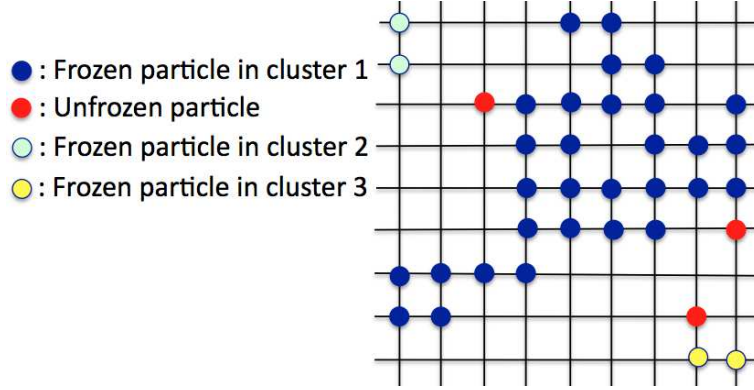


Fig. 9 (Color online) Frozen particles and clusters. The configurations outside of the figures are assumed to be consistent.

Appendix: Sketch of the proof for the absence of locally frozen particles

In section 3.1, we assumed the fact that the clusters of frozen particles in the bulk are always constrained partly by the boundary sites. In order to explicitly state such an argument, as preliminary, we start with the following definitions and will give a sketch of the proof for the argument.

Definition 0 (frozen particles): $\mathcal{F}_{\text{all}}(\sigma)$ denotes a set of all the frozen sites (particles) for a given configuration σ , where for $\forall i \in \mathcal{F}_{\text{all}}$, site i is constrained only by sites in \mathcal{F}_{all} and boundary sites. \mathcal{B}_d denotes a set of boundary sites.

Definition 1 (frozen cluster): $\mathcal{F} \subset \mathcal{F}_{\text{all}}$ denotes a set “frozen cluster” of frozen particles, where for $\forall i \in \mathcal{F}$, $\exists j \in \mathcal{F} \cup \mathcal{B}_d$ such that $|i - j| \leq 3$ and (maximum property) for $\forall k \notin \mathcal{F}$, $k \cup \mathcal{F}$ is not a frozen cluster. See figure 9 for helping to imagine the frozen particles and frozen clusters.

Definition 2 (frozen links): $\mathcal{L}(\mathcal{F})$ denotes a set of “frozen links” for \mathcal{F} , consisting of straight line segments (i, j) between i and j for $\forall i, j \in \mathcal{F}$.

Definition 3 (outer sites): $\overline{\mathcal{F}}$ denotes a set of outer sites for \mathcal{F} , where for $\forall i \in \overline{\mathcal{F}}$, i has a path to a boundary site without crossing $\forall k \in \mathcal{L}(\mathcal{F})$.

Definition 4 (outer links): $\partial\mathcal{L}(\mathcal{F})$ denotes a set of outer links, where arbitrary points on $k \in \partial\mathcal{L}(\mathcal{F})$ has a path to a boundary site without crossing $\forall k \in \mathcal{L}(\mathcal{F})$.

Definition 5 (edge sites): $\partial\mathcal{F} \equiv \mathcal{F} \cap \overline{\mathcal{F}}$ is a set of edge sites. By the definition of edge sites and outer links, for $\forall (i, j) \in \partial\mathcal{L}(\mathcal{F})$, $i, j \in \partial\mathcal{F}$. See figure 10 for helping to image outer sites, outer links, and edges sites.

On the basis of those definitions, one can obtain the following property:

Geometric property 1: The figure generated by all the outer links in $\partial\mathcal{L}(\mathcal{F})$ are locally convex toward \mathcal{F} .

Assume that the figure generated by $(i, j), (j, k) \in \partial\mathcal{L}(\mathcal{F})$ is not convex toward \mathcal{F} . Then, one can construct another outer link connecting i and k , and $(i, j), (j, k) \notin \partial\mathcal{L}(\mathcal{F})$ by the definition of the outer links. This contradiction immediately leads to *Geometric property 1*.

By the local convexity in *Geometric property 1*, one may immediately conclude the following property:

Geometric property 2: The figure generated by all the outer links in $\partial\mathcal{L}(\mathcal{F})$ is a convex polygon or a convex polyline toward \mathcal{F} .

Finally, we explicitly state about the absence of locally frozen particles in the following.

Statement: There exist frozen particles constrained by the boundary sites for arbitrary frozen clusters: For $\forall \mathcal{F} \neq \emptyset$, $\exists i \in \mathcal{F}$ such that $\min_{j \in \mathcal{B}_d} |i - j| \leq 3$.

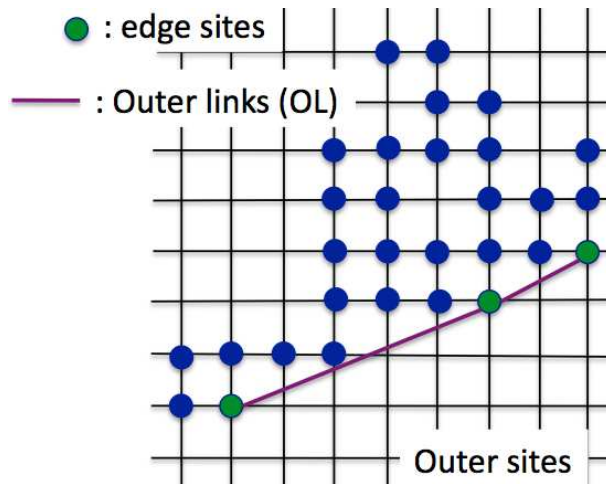


Fig. 10 (Color online) Outer sites, outer links, and edges sites. The configurations outside of the figures are assumed to be consistent.

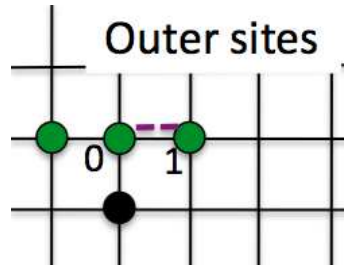


Fig. 11 (Color online) The case with 3 particles at sites in B_0 . In this case, the slope of outer links $(0, 1) \in \partial\mathcal{L}(\mathcal{F})$ clearly does not change, comparing to the previous outer link. As far as the edge sites continue to have three particles at the nearest neighbors, this situation does not change.

Sketch of the proof: Assume that there exists a frozen cluster \mathcal{F} such that $\forall i \in \mathcal{F}, \min_{j \in \mathcal{B}_d} |i - j| > 3$. Then let us consider what kinds of configuration could appear near edge sites in $\partial\mathcal{F}$. Remembering the *maximum property* of frozen clusters, one can easily find that each site in $\partial\mathcal{F}$ has at least two particles, but less than four particles at the nearest neighbors. The case with three particles is illustrated in figure 11, and it can be seen that one immediately has to consider the case with two particles.

Thus, we focus on the case with two particles at the nearest neighbor of an edge site. According to *Geometric property 1*, one can illustrate two possible and nontrivial configurations as illustrated in figure 12. Concretely, we first pick up an edge site 0 in $\partial\mathcal{F}$, and consider the slope of outer links $(0, k) \in \partial\mathcal{L}(\mathcal{F})$ to curve downward in order to make a polygon, without loss of generality because one has to consider these cases in the end at the latest. However, it turns out that the slope of outer links $(0, k) \in \partial\mathcal{L}(\mathcal{F})$ in both configurations cannot be changed to make any polygons (see the caption in figure 12). Note that the cases where there is a particle at site a or b to make site 0 constrained are also possible, but the slope of the outer link $(0, k) \in \partial\mathcal{L}(\mathcal{F})$ does not change downward at all. As explained in the caption of figure 12, those cases are enough to consider impossibility for the outer links to make them being a polygon base on the assumption we have made. Therefore, one may conclude that the figure generated by all the outer links in $\partial\mathcal{L}(\mathcal{F})$ is not a polygon on the assumption we have made.

Therefore, another possibility is that the figure generated by all the outer links in $\partial\mathcal{L}(\mathcal{F})$ is a convex polyline according to *Geometric property 2*. However, in this case, the tip of the line has to be constrained by a boundary site because the tip of the line should have at least one more particle at the nearest neighbors by the definition. Thus, one may conclude there are contradictions, leading to *Statement*.

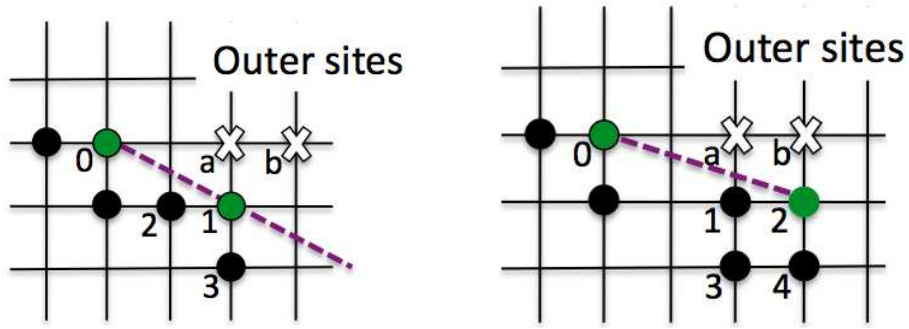


Fig. 12 (Color online) The situations where an edge site 0 has two particles in B_0 and a particle at site 1 makes site 0 constrained (a and b are outer sites in $\overline{\mathcal{F}}$). It is necessary to consider these rather particular situations because even if we consider the cases where site 0 is constrained by the other sites such as sites a and b , one clearly has to consider these situations again in order to make a polygon. (left) Assume that site 1 is an edge site in $\partial\mathcal{F}$. In this case, the situation that there are particles at sites 2 and 3 is only the possibility to be consistent with the definitions made in the text. Finally, the edge site 1 has the same situation as that of site 0. Therefore, The slope of outer link $(0, 1)$ cannot become sharper than that of the next outer link $(1, k) \in \partial\mathcal{L}(\mathcal{F})$. (right) Assume that site 1 is not an edge site. In this case, there must exist a particle at site 2. Assume that site 2 is an edge site in $\partial\mathcal{F}$. In this case, the situation that there are particles at sites 1 and 4, is only the possibility to be consistent with the definitions made in the text. Finally, the edge site 2 has the same situation as that of site 0, and the slope of outer link $(0, 2)$ is not sharper than that of outer link $(0, 1)$. Finally, if one consider the last possibility that site 2 is not an edge site, the slope of the outer link $(1, k) \in \partial\mathcal{L}(\mathcal{F})$ cannot be sharper than that of outer link $(0, 2)$ by the definition of the outer links. Concretely, this is because if the slope of outer link $(1, k)$ would be sharper than that of outer link $(0, 2)$, site 2 would be an edge site, which leads to the contradiction.